Eur. Phys. J. C 11, 661–672 (1999)
Digital Object Identifier (DOI) 10.1007/s100529900217

THE EUROPEAN PHYSICAL JOURNAL C

Implications of the precision data for very light Higgs Boson scenarios in 2HDM(II)

P.H. Chankowski[1,2], M. Krawczyk[2], J. Żochowski[2]

[1] Theory Division, CERN, Geneva, Switzerland
[2] Institute of Theoretical Physics, Warsaw University, Poland

Received: 8 June 1999 / Published online: 14 October 1999

Abstract. We present an up-to-date analysis of the constraints the precision data impose on the ($CP-$conserving) Two Higgs Doublet Model of type II with emphasis on the possible existence of very light neutral (pseudo)scalar Higgs boson with mass below $20-30\,\mathrm{GeV}$. We show that even in the presence of such light particles, the 2HDM(II) can describe the electroweak data with the precision comparable to that given by the SM. Particularly interesting lower limits on the mass of the lighter neutral $CP-$even scalar h^0 are obtained in the scenario with light $CP-$odd Higgs boson A^0 and large $\tan\beta$.

1 Introduction

The Standard Model (SM) of electroweak interactions is in very good agreement with the electroweak precision data collected at LEP and SLAC experiments [1]. This fact strongly supports the idea of the spontaneous breaking of the underlying $SU_L(2)\times U_Y(1)$ gauge symmetry. Yet, the actual mechanism of symmetry breaking remains still unexplored. The Higgs boson predicted by the minimal model of electroweak symmetry breaking, the SM, has not been found up to now. Only the lower limit on its mass of $\sim 90\,\mathrm{GeV}$ is set by the unsuccesful search at LEP. While the Higgs sector of the SM is theoretically appealing due to its extreme simplicity, there exist many of its extensions which lead to different phenomenology (more physical Higgs particles) and which also should be tested (or constrained) experimentally.

The simplest such an extension is the well known two Higgs doublet model (2HDM). It exists in several distinct versions of which we want to consider in this letter the one, called the Model II in its $CP-$conserving version (we briefly recall its structure in the next Section).[1] One interesting question which arises in the context of such an extension of the SM is what are the available experimental limits on masses of the Higgs bosons predicted in such a model. In Sect. 3 we will recall the arguments [2] that, in the framework of the considered version of 2HDM, the direct searches do not exclude the existence of very light neutral scalar or pseudoscalar Higgs particles. In Sect. 4 we show that the existence of such light Higgs bosons is neither excluded by the electroweak precision data. Analysis of the impact of the precision data on the 2HDM(II) has already been performed in the past [6, 3] (for the formalism and early investigations see also [4]) but concentrated mainly on the possibility of improving the prediction for $R_b\equiv\Gamma(Z^0\to\bar{b}b)/\Gamma(Z^0\to hadrons)$ (which at that time seemed to be required by the data) and on improving the 2HDM(II) global fit to the data with respect to the fit given by the SM. Since then, the experimental situation has evolved significantly. In particular the measurement of R_b no longer shows any statistically significant deviation from the value predicted by the SM [1]. Also there are changes both in the experimental measurement and theoretical computation of the $b\to s\gamma$ decay rate which was crucial in the analysis performed in [3]. More recently a partial analysis of the constraints iposed on the 2HDM(II) by various measurements has been also attempted in [5]. Here we present an up-to-date analysis of the constraints the precision data impose on the 2HDM(II) with emphasis on the possible existence of light neutral (pseudo)scalar Higgs boson. We show that even in the presence of such light particles, the 2HDM(II) can describe the electroweak data with the precision comparable to that given by the SM. In this case some interesting global limits on the model can be obtained. Finally in Sect. 5 we summarize our results and briefly comments on the other ways the existence of light Higgs bosons are or can be constrained by other expermental data.

[1] The Higgs sector of the Minimal Supersymmetric Standard Model has precisely the structure of the Model II but with additional constraints imposed on the quartic couplings. However, in the following we will consider the general Model II in a regime in which it cannot be regardeded as a low energy approximation to the MSSM with heavy sparticles

2 Two Higgs doublet extension of the SM – Model II

The multi-doublet extensions of the SM are distinguished by their virtue of not introducing corrections to the ρ parameter at the tree level. The minimal extension of the SM consist of two doublets. The requirement of the absence at the tree level of the flavour changing neutral currents puts restrictions on how the two scalar doublets of the general 2HDM can couple to fermions. In the Model II, one Higgs doublet (denoted by Φ_1) couples only to leptons and down-type quarks whereas the other doublet (Φ_2) couples only to up-type quarks. After spontaneous symmetry breaking both doublets acquire vacuum expectation values v_1 and v_2, respectively with $v \equiv \sqrt{v_1^2 + v_2^2}$ fixed by M_W, and

$$\frac{v_2}{v_1} \equiv \tan\beta. \tag{1}$$

With two complex Higgs doublets, the 2HDM predicts the existence of five physical scalars: neutral h^0, H^0 and A^0 and charged $H^\pm$. In the more restrictive scenario (which we are going to discuss) with CP symmetry conserved by the Higgs potential, h^0 and H^0 are $CP-$even mixtures of the neutral components of the doublets (the mixing being parametrized by the angle α) whereas A^0 is $CP-$odd. Thus, in the $CP-$conserving version, the Higgs sector is parametrized by four masses M_h, M_H (by definition $M_h \leq M_H$), M_A and M_{H^+} and three dimensionless parameters $\tan\beta$, α and λ_5 (for definitions see eg. [7]). The first two dimensionless parameters are very important for the phenomenology of the Higgs sector as they determine the couplings of the physical Higgs bosons to fermions and gauge bosons: the couplings of the scalars to the down- and up- type quarks are given by the SM couplings multiplied by the factors (see e.g. [7,8])

$$\begin{aligned}
h^0 b\bar{b}: &\ -\frac{\sin\alpha}{\cos\beta} = \sin(\beta-\alpha) - \tan\beta\cos(\beta-\alpha)\\
h^0 t\bar{t}: &\ \frac{\cos\alpha}{\sin\beta} = \sin(\beta-\alpha) + \cot\beta\cos(\beta-\alpha)\\
H^0 b\bar{b}: &\ \frac{\cos\alpha}{\cos\beta} = \cos(\beta-\alpha) + \tan\beta\sin(\beta-\alpha)\\
H^0 t\bar{t}: &\ \frac{\sin\alpha}{\sin\beta} = \cos(\beta-\alpha) - \cot\beta\sin(\beta-\alpha).
\end{aligned} \tag{2}$$

The Feynman rules for the $CP-$odd scalar couplings to fermions are given by the SM rules for h^0_{SM} times the factors:

$$A^0 b\bar{b}: \ -i\gamma^5\tan\beta, \quad A^0 t\bar{t}: \ -i\gamma^5\cot\beta. \tag{3}$$

Important for the direct Higgs boson search at LEP couplings $Z^0Z^0h^0$ and $Z^0Z^0H^0$ are given by the corresponding Standard Model coupling $Z^0Z^0h^0_{SM}$ modified by the factors:

$$Z^0Z^0h^0: \ \sin(\beta-\alpha), \quad Z^0Z^0H^0: \ \cos(\beta-\alpha) \tag{4}$$

whereas the couplings of Z^0 to A^0h^0 and A^0H^0 pairs are instead proportional to

$$Z^0A^0h^0: \ \cos(\beta-\alpha), \quad Z^0A^0H^0: \ \sin(\beta-\alpha). \tag{5}$$

It follows, that in the limit $\sin(\beta-\alpha) = 1$ the lighter $CP-$even neutral Higgs boson h^0 has precisely the couplings of the Standard Model Higgs and becomes indistinguishable from it. Finally, couplings of the charged Higgs scalar to fermions, e.g. $\bar{b}tH^-$ vertex, are given by expressions like:

$$\frac{g}{2\sqrt{2}M_W}\left[m_t\cot\beta(1+\gamma_5) + m_b\tan\beta(1-\gamma_5)\right].$$

It is clear that for $\tan\beta$ close to zero, scalar couplings to $t\bar{t}$ pairs are strongly enhanced compared to the SM case, whereas for $\tan\beta$ large ($\gtrsim 10$) enhanced are couplings to $b\bar{b}$. Requirement of perturbativity of both type of couplings restricts, therefore, $\tan\beta$ values to the range [9]:

$$0.3 \lesssim \tan\beta \lesssim 130. \tag{6}$$

Outside this range perturbativity is lost and no firm prediction can be obtained from the model.

3 Constraints on the 2HDM(II) from direct Higgs boson search at LEP

Here we briefly review the constraints on the 2HDM(II) imposed by direct Higgs boson search at LEP [2], which will be taken into account in performing the fits to the electroweak data in Sect. 4. At LEP e^+e^- collider the Higgs boson search is based mainly on the following processes:

1. the Bjorken process $e^+e^- \to Z^{0\star}h^0(H^0)$
2. the associated Higgs boson pair production $e^+e^- \to A^0h^0(H^0)$
3. the Yukawa process $e^+e^- \to b\bar{b} \to b\bar{b}A^0(h^0)$
4. $e^+e^- \to H^+H^-$.

Due to the structure of the $Z^0Z^0h^0$ and $Z^0A^0h^0$ couplings (4,5) the processes $e^+e^- \to Z^{0\star}h^0$ and $e^+e^- \to A^0h^0$ are complementary to each other provided they are simultaneously kinematically allowed. In the SM, or in the 2HDM(II) in the limit $\sin(\beta-\alpha) = 1$, the nonobservation of the Bjorken process at LEP sets the lower limit on $M_{h_{SM}}$ of $\sim 90\,\mathrm{GeV}$ (at 95% C.L.) [10]. In the general case, the same data put an upper limit on the factor $\sin^2(\beta-\alpha)$ as a function of the lighter Higgs boson mass M_h (see Fig. 1). The combined analysis of the complementary channels 1. and 2. performed e.g. by the OPAL collaboration [15] leads the the constraints on the $(M_h,\ M_A)$ plane shown in Fig. 2. It follows that the direct experimental limits on M_h and M_A are rather weak: the data allow for very light h^0 (A^0) provided A^0 (h^0) is heavier than ~ 65 (50) GeV even if only $\tan\beta > 1$ is allowed. In particular, no absolute bound on M_h from LEP data exists provided one respects the bound on $\sin^2(\beta-\alpha)$ shown in Fig. 1.

For large values of $\tan\beta$ independent constraints on h^0 and A^0 follow from the nonobservation of the Yukawa process. The available limits on the $(M_A, \tan\beta)$ plane are shown in Fig. 3 [15]. Similar limits on both, $(M_h, \tan\beta)$

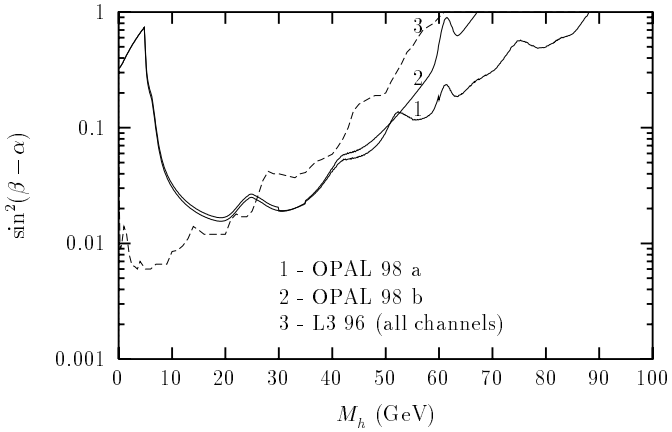

Fig. 1. 95% C.L. limits on $\sin^2(\beta-\alpha)$ from the Higgs boson search at LEP as a function of M_h. Lines 1 and 2 are the OPAL results obtained assuming the Higgs boson decay branching ratios as in the SM and 100% into hadrons, respectively [11]. Line 3 is the result of L3 [12]

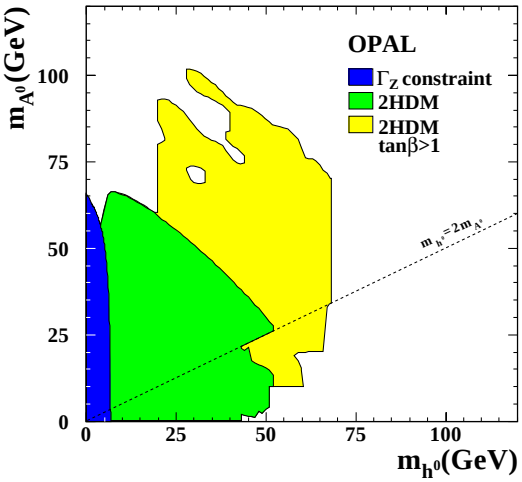

Fig. 2. 95% C.L. limits on $(M_h,\ M_A)$ plane from the Bjorken process and the associated Higgs boson production as given by the OPAL collaboration [15]

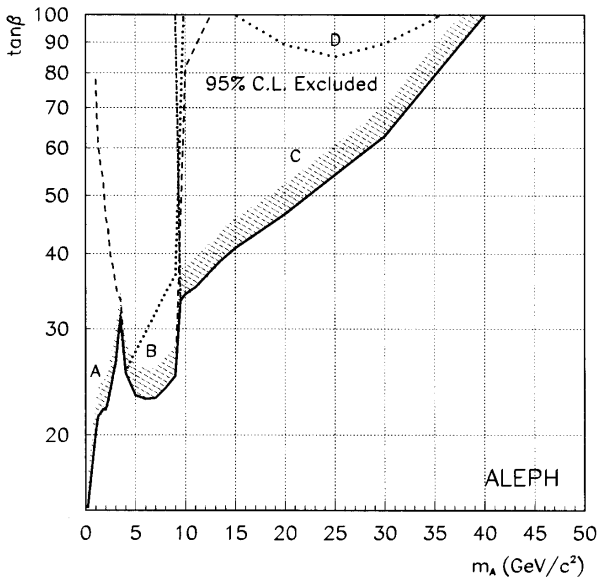

Fig. 3. 95% C.L. limits on $(\tan\beta,\ M_A)$ plane from the Yukawa process as given by the ALEPH collaboration [15]

and $(M_A, \tan\beta)$ planes have been reported only recently by the DELPHI Collaboration [16].

It should be also mentioned that some, rather weak (and dependend on the assumptions made about the Higgs boson decay branching fractions) limits on the very light h^0 and A^0 can be derived from the so-called Wilczek processes [13] i.e. from Υ and J/ψ decays into $h^0(A^0)$ and the photon [14]. We do not take these limits into account in performing the fit to the electroweak data because the results we will show do not change as M_h varies over the range $0-30\,\mathrm{GeV}$. It should be also clear that whenever $\sin^2(\beta-\alpha)\approx 0$ the heavier $CP-$even scalar, H^0, is constrained by the Bjorken process so that $M_H \gtrsim 90\,\mathrm{GeV}$. Finally, the nonobservation of the charged Higgs boson production at LEP sets the bound $M_{H^+} > 72\,\mathrm{GeV}$ [17] which is, however, much less restrictive than the indirect limit derived in the 2HDM(II) from the $b\to s\gamma$ process and, for $\tan\beta<1$, from R_b.

From the above it follows that within the 2HDM(II) there still exist two scenarios with either very light scalar h^0 or very light pseudoscalar A^0 which are not excluded by the available data (for other constraits not discussed here see [32,33] and Sect. 5).

In the next Section we will consider how the electroweak precision data constrain these two scenarios.

4 Global fit to the precision data

Since the advent of LEP and SLAC experiments, precision electroweak data have been playing increasingly important rôle in constraining the mass of the top quark in the Standard Model (SM). Nowadays, with the top quark mass directly measured at Fermilab [18], they constrain significantly the last unknown parameter of the SM, the mass of the Higgs boson [19]. They are also very useful in constraining possible forms of new physics such as supersymmetry [20] or technicolor [21]. It is, therefore, natural to ask to what extent the precision electroweak data constrain the Two Higgs Doublet Model of the type II. In this context, the question of particular importance is whether they are still compatible with the existence of a very light neutral Higgs particle (scalar or pseudoscalar one) which, as we discussed in the preceding Section, is not yet excluded by direct searches. In this Section we discuss under what conditions the existence of light h^0 or A^0 can be compatible with indirect constraints imposed by precision data.

Strictly statistical approach to constraining the 2HDM(II) indirectly would consist of finding the global minimum of the χ^2 fit and, in the next step, excluding all points in the parameter space for which $\Delta\chi^2$ is greater than 3.84 (exclusion at 95% C.L.). Comparison of such an analysis with the similar one carried for the SM would re-

veal that, per degree of freedom (d.o.f.), the fit in 2HDM(II) is much worse than in the SM. This follows from the fact that the description of the electroweak data by the latter is nearly perfect [1]. Hence, the 2HDM(II) predicting individual observables as accurately as the SM would have much worse χ^2/d.o.f. because of larger number of free parameters in its Higgs potential. In our investigation we do not follow such an approach. Rather, we take the SM best global χ^2 value as a reference point and concentrate on the qualitative discussion of which regions of the 2HDM(II) parameter space can give equally good global χ^2 value. In order not to be too restrictive, when constraining the parameter space we use the rough criterion that the χ^2 in the 2HDM(II) should not be greater than the SM best χ^2 value plus 4. Our emphasis is however on the fact that such a criterion (in fact any reasonable one) does allow for a very light neutral scalar or pseudoscalar. The data we take into account include the precision electroweak data reported at the Moriond'98 conference [1], which are dominated by those from LEP 1. For future reference we record that the best SM fit to the electroweak data we have chosen gives us $\chi^2 \approx 15.5$. Therefore, all bounds on the masses of the 2HDM(II) Higgs bosons we will present are derived by requiring the χ^2 in that model to be less than 19.5.

In discussing the values the χ^2 takes for various Higgs boson mass configurations (to explain qualitatively the origins of the bounds we show) we will always start with the discussion of the contribution to the $\Delta\rho$ parameter defined as

$$\Delta\rho = \frac{\Pi_{WW}(0)}{M_W^2} - \frac{\Pi_{ZZ}(0)}{M_Z^2} - 2\frac{s_W}{c_W}\frac{\Pi_{Z\gamma}(0)}{M_Z^2}, \qquad (7)$$

where s_W (c_W) is the sine (cosine) of the Weinberg angle. It determines largely the bulk of the predicted in the model values of the electroweak observables like M_W, $\sin^2\theta^{eff}$ (measured through various asymmetries of the final fermions and/or their polarizations [1]) etc. and is therefore the main factor shaping the χ^2 curves, at least for not too small or too large values of $\tan\beta$ i.e. when the couplings of the Higgs bosons to the $b\bar{b}$ pair are not enhanced.

In addition, for low and high values of $\tan\beta$ particularly important rôle in the fit is played by the quantity R_b. The current experimental result is $R_b = 0.21656$ with the error $\Delta R_b = 0.00074$ (which is 0.9 standard deviation above the SM prediction). Its importance follows from the fact that in the 2HDM(II) the contribution of the Higgs bosons can easily change the prediction for R_b compared to the SM, spoiling the χ^2 fit to the data. This contribution has been studied in detail in [22]. (Handy formulae for δR_b can be also found in the Appendix of [23].) The contribution of H^+ to δR_b contains parts proportional to $(m_t/M_Z)^2\cot^2\beta$ and $(m_b/M_Z)^2\tan^2\beta$ and, consequently, can be sizeable for either very small or very large values of $\tan\beta$. The neutral scalars become relevant for R_b only in the latter limit (see (2,3)). For a qualitative understanding of the results it is sufficient to remember that the contribution of H^+ is always negative, whereas the contribution of the neutral Higgs bosons can be positive provided A^0 is not too heavy, say $M_A \lesssim 100\,\mathrm{GeV}$, and the splitting between its mass and the mass of the $CP-$even scalar h^0 or H^0 (the one which for a given angle α couples more strongly to the $b\bar{b}$ pair) is not too large. For example, in the configuration (typical for the Minimal SUSY Standard Model with large $\tan\beta$) $M_h \sim M_A \lesssim 70\,\mathrm{GeV}$ (and $\sin^2\alpha \approx 1$) the contribution of A^0 and h^0 can easily overcompensate the negative contribution of H^+ with mass $M_{H^+} > 100\,\mathrm{GeV}$. It is the interplay of the contribution to the $\Delta\rho$ parameter and the contribution to δR_b which is responsible for interesting bounds on 2HDM(II) with light (pseudo)scalar particle which can be derived on the basis of the χ^2 fit.

Another very important constraint on new physics is the measured value of the branching ratio $BR(B \to X_s\gamma)$ [24]. In the context of the 2HDM(II) this measurement can be converted into a lower bound on the mass of the charged Higgs boson [25]. Recently there was a big effort of various groups to improve the accuracy of the theoretical prediction for this ratio [26–28]. Our lower bound on M_{H^+} based on $b \to s\gamma$ for $m_t = 174\,\mathrm{GeV}$ is shown as a function of $\tan\beta$ in Fig. 6a by the solid line. [2] It is (for large $\tan\beta$) higher by some 35 GeV than the recent estimate [30] which gives $M_{H^\pm} \gtrsim 165\,\mathrm{GeV}$. In view of the well known exquisite sensitivity of the limit on M_{H^+} on the details of the analysis this should be considered as a satisfactory agreement. We will, however, try to keep open the possibility that the charged Higgs boson can be as light as $\sim 165\,\mathrm{GeV}$.

4.1 Light h^0

We discuss the light h^0 scenario first. For the sake of clarity it is convenient to distinguish two h^0 mass ranges: *i)* $M_h \lesssim 30\,\mathrm{GeV}$, and *ii)* $M_h > 30\,\mathrm{GeV}$. This division follows from the upper bounds imposed by the direct LEP search on the allowed value of $\sin^2(\beta-\alpha)$ [12] (Fig. 1): in the case *i)* $\sin^2(\beta-\alpha) < 0.01 - 0.02$ (and for practical purposes can be set to zero); in the case *ii)* the upper bound on $\sin^2(\beta-\alpha)$ changes roughly linearly (on the logarithmic scale) from ~ 0.02 for $M_h \approx 30\,\mathrm{GeV}$ up to 1 for $M_h \approx 90\,\mathrm{GeV}$ (see Fig. 1). In this paper we will be mainly interested in case *i)* and will essentially not explore the case *ii)* which requires more involved analysis. It will also prove helpful to consider separately two ranges of the parameter $\tan\beta \equiv v_2/v_1$, namely $0.5 \lesssim \tan\beta \lesssim 10 - 20$ (small and intermediate) and $20 \lesssim \tan\beta \lesssim 50$ (large).

[2] We compute $BR(b \to s\gamma)$ with NLO accuracy following the approach of [29] supplemented with electromagnetic as well as $1/m_b^2$ and $1/m_c^2$ corrections setting the parameter $\delta = 0.9$ [28]. The theoretical uncertainty is taken into account by computing the rate for $\mu_b = 2.4$ and 9.6 GeV and then by shifting its larger (smaller) value upward (downward) by the added in quadratures errors related to the uncertainties in α_s, m_b, m_c/m_b, $|V_{tb}V_{ts}^\star/V_{cb}|^2$, and higher order electroweak corrections; we do not take into account the variation of the scale μ_W. If the resulting band of theoretical predictions for $BR(b \to s\gamma)$ has an overlap with the CLEO 95% C.L. band the point is allowed

Distinct properties of these regions follow from different sensitivity of the important observable R_b to the masses of the Higgs bosons for small and intermediate, and for large $\tan\beta$ values.

In order to understand qualitatively the main features of the χ^2 fit to the electroweak data it is instructive to begin the discussion of the light h^0 case with the somewhat peculiar limit in which the remaining Higgs bosons, $H^\pm$, A^0 and H^0, are exactly degenerate and have a common mass M_D. In Fig. 4a we show the value of χ^2 obtained in the 2HDM(II) as a function of M_h for different values of $\tan\beta$ and $M_D = 250\,\mathrm{GeV}$. Corresponding values of R_b are shown in Fig. 4b. In both cases we set $\sin^2(\beta-\alpha)=0$ and we keep fixed $m_t = 174\,\mathrm{GeV}$. The pattern observed in Fig. 4a can be easily understood by checking the contributions to the parameter $\Delta\rho$ which in the 2HDM [7] can be represented in the convenient form:

$$\Delta\rho = \frac{\alpha}{4\pi s_W^2 M_W^2} A(M_A, M_{H^+}) + \cos^2(\beta-\alpha)\Delta_c + \sin^2(\beta-\alpha)\Delta_s \qquad (8)$$

where

$$\Delta_c = \frac{\alpha}{4\pi s_W^2 M_W^2}\left[A(M_{H^+}, M_h) - A(M_A, M_h)\right] + \Delta\rho_{SM}(M_H) \qquad (9)$$

and Δ_s is obtained by the exchange $M_h \leftrightarrow M_H$. The function

$$A(x,y) = A(y,x) \equiv \frac{1}{8}x^2 + \frac{1}{8}y^2 - \frac{1}{4}\frac{x^2y^2}{x^2-y^2}\log\frac{x^2}{y^2} \qquad (10)$$

is positive and large if $x \gg y$ and vanishes for $x = y$. Finally,

$$\Delta\rho_{SM}(M) = \frac{\alpha}{4\pi s_W^2 M_W^2}\left[A(M,M_W) - A(M,M_Z)\right] + \frac{\alpha}{4\pi s_W^2} \times \left[\frac{M^2}{M^2-M_W^2}\log\frac{M^2}{M_W^2} - \frac{1}{c_W^2}\frac{M^2}{M^2-M_Z^2}\log\frac{M^2}{M_Z^2}\right] \qquad (11)$$

is the Standard Model Higgs boson contribution to $\Delta\rho$. Good quality of the fit is obtained for

$$\Delta\rho_{NEW} = \Delta\rho - \Delta\rho_{SM}(M_{h^0_{SM}}) \approx 0 \qquad (12)$$

where $M_{h^0_{SM}}$ is a reference SM Higgs boson mass $\approx 100\,\mathrm{GeV}$.

Since in the case of triple degeneracy shown in Fig. 4 $\Delta\rho$ is independent of $\tan\beta$, $\sin^2(\beta-\alpha)$ and M_h values, for fixed M_D the χ^2 curves reflect mainly[3] the dependence of R_b on M_h for different values of $\tan\beta$. For low and moderate values of $\tan\beta$ the predicted value of R_b is M_h independent, whereas for large $\tan\beta$ ($\gtrsim 20$), for which the $h^0 b\bar{b}$ coupling is enhanced (see Eq. 2), the sensitivity of R_b to M_h becomes crucial. In addition, for light H^+ (i.e. small M_D, $\sim 200\,\mathrm{GeV}$) its negative contribution to R_b spoils the χ^2 fit for very small or very large values of $\tan\beta$ (but this effect is M_h independent). On the top of that comes, the global sensitivity of the fit to M_D which enters through $\Delta\rho_{SM}(M_D)$. This dependence is exactly the same as the dependence of the SM fit (for fixed top quark mass) on the value of the SM Higgs boson mass. It follows that the best fit (in the case of triple degeneracy) is obtained for M_D as low as possible and intermediate values of $\tan\beta$. Note that only the case of $M_D = 250\,\mathrm{GeV}$ and $\tan\beta = 5$ (and marginally, for heavier h^0, also for $\tan\beta = 20$) shown in Fig. 4 yields acceptable value of χ^2. Allowing for $M_D = 165\,\mathrm{GeV}$ gives (for intermediate values of $\tan\beta$) $\chi^2 \approx 17.5$. In the region *i)* taking $\sin^2(\beta-\alpha) = 0.01$ improves χ^2 only marginally (it decreases by ~ 0.2 for $M_D = 250\,\mathrm{GeV}$). In the region *ii)* taking the largest allowed by the LEP data value of $\sin^2(\beta-\alpha)$, e.g. $\sin^2(\beta-\alpha) = 0.2$ for $M_h = 50\,\mathrm{GeV}$ decreases for $M_D = 250\,\mathrm{GeV}$ the χ^2 value to ~ 18.1 as a result of "redistribution" of contributions in the last two terms in (8).

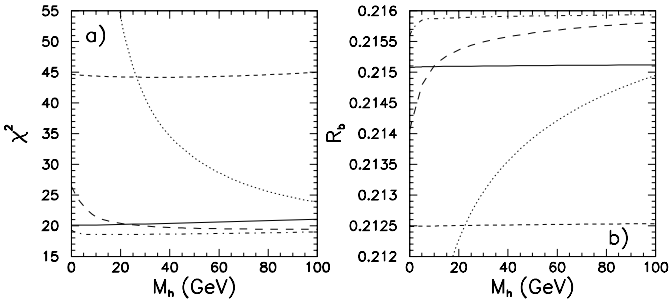

Fig. 4a,b. χ^2 and R_b as a function of M_h in the case of triple degeneracy with $M_D \equiv M_H = M_A = M_{H^+} = 250\,\mathrm{GeV}$ and $\sin^2(\beta-\alpha) = 0$. Short-dashed, solid, dot-dashed, long-dashed and dotted lines correspond to $\tan\beta$ =0.5, 1, 5, 20 and 50, respectively. The top mass is fixed to $m_t = 174\,\mathrm{GeV}$

Essential improvement of the fit is, however, obtained by the departure from the strict limit of triple degeneracy. For very small and intermediate values of $\tan\beta$ this is illustrated in Fig. 5 where for $M_h = 20\,\mathrm{GeV}$ (which is representative for $0 < M_h \lesssim 30\,\mathrm{GeV}$), $\sin^2(\beta-\alpha) = 0$ and fixed $m_t = 174\,\mathrm{GeV}$ we show χ^2 as a function of M_A for different combinations of H^+ and H^0 masses.

To explain the pattern of χ^2 seen in Figs. 5a for $\tan\beta = 2$ (which is representative for intermediate values of $\tan\beta$ for which the predicted value of R_b is as in the SM), recall that the SM-type contribution (11) to $\Delta\rho$, eq. (8), is negative and (for $\sin^2(\beta-\alpha) = 0$) decreases with increasing H^0 mass. This too negative contribution can be easily compensated for by the contribution of the other Higgs bosons to $\Delta\rho$ when the equality of H^0, H^+ and A^0 masses is relaxed. From (8-9) it follows that their contribution is positive provided $M_{H^+} \gtrsim M_A$. Obviously, $M_{H^+} - M_A$ mass splitting must increase with increasing M_H in order to compensate for increasingly negative H^0 contribution to $\Delta\rho_{SM}$. It is also clear that the possibility to adjust total $\Delta\rho$ to a proper value should hold also for larger M_h and/or $\sin^2(\beta-\alpha) \neq 0$. We have checked that for example, for

[3] For qualitative explanation of the shapes of the χ^2 curves the other "oblique" parameters, S and U, [31] play only a secondary rôle

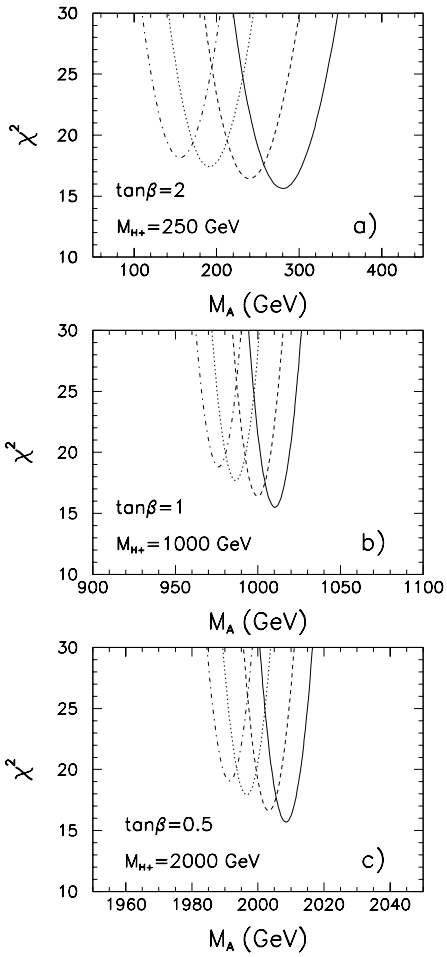

Fig. 5a–c. χ^2 for $M_h = 20\,\mathrm{GeV}$ and $\sin^2(\beta-\alpha) = 0$ as a function of M_A for different low and intermediate values of $\tan\beta$ and different H^+ masses. Solid, dashed, dotted and dot-dashed lines correspond to M_H =90, 200, 500 and 1000 GeV, respectively. $m_t = 174\,\mathrm{GeV}$

$M_h = 50\,\mathrm{GeV}$ and $\sin^2(\beta-\alpha) = 0.2$ (see Fig. 1) the plots look very similar as for $M_h = 20\,\mathrm{GeV}$ and $\sin^2(\beta-\alpha) = 0$.

Because the contribution of H^+, A^0 and h^0 to $\Delta\rho$ depends on differences of the masses squared (quadratic violation of the $SU_V(2)$ "custodial" symmetry) the cancelation between their contribution and $\Delta\rho_{SM}$ needed in the case of $M_h \lesssim 20\,\mathrm{GeV}$ to adjust $\Delta\rho$ to a proper value becomes more and more delicate as the mass of M_{H^+} increases. This leads to stronger and stronger correlation of M_{H^+} with M_A clearly seen in Figs. 5 (note different mass scales in the panels). This correlation becomes particularly fine-tuned in the case of small $\tan\beta$ where the requirement of good R_b forces M_{H^+} to be large. The lower limits imposed on M_{H^+} by $b \to s\gamma$ and R_b are shown in Fig. 6a by the solid and dashed lines respectively. Since the very strong correlation of M_{H^+} with M_A may seem unnatural it is interesting to see how the requirement of "naturalness" of the χ^2 constrains the parameter space. This is illustrated by the dotted (dash-dotted) line in Fig. 6a which bounds from below the region in the ($\tan\beta$, M_{H^+}) plane in which a change of M_A by $\lesssim$1% (3%) from its

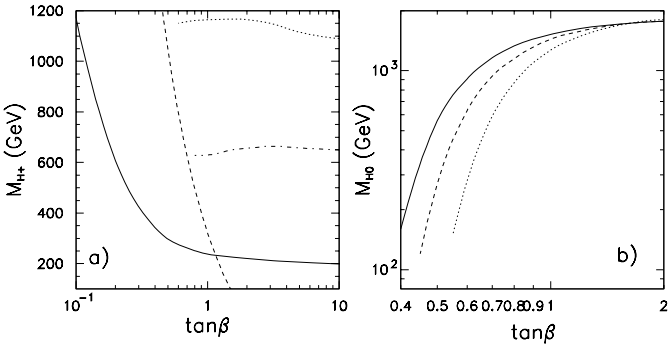

Fig. 6. a Lower limits on H^+ mass coming separately from $b \to s\gamma$ (solid line) and from the requirement that $R_b^{2HDM} > R_b^{EXP} - 2(\Delta R_b)^{EXP}$ (dashed line) as a function of $\tan\beta$. Also shown are upper limits on M_{H^+} arising for $M_h < 20\,\mathrm{GeV}$ from the requirement of fine tuning in M_A not larger than 1% and 3% (dotted and dash-dotted lines, respectively). **b** Upper limits on M_H in the case of light h^0 ($M_h \leq 20 - 30\,\mathrm{GeV}$; $\sin(\beta-\alpha) = 0$) and $M_{H^+} = 1000$, 800 and 600 GeV (solid, dashed and dotted lines, respectively)

value giving the minimum of χ^2 (for that particular point in the ($\tan\beta$, M_{H^+}) plane) does not lead to $\chi^2 > 19.5$. In producing these curves the fit was always optimized with respect to the values of M_H and m_t.[4] It is also interesting to note (see Figs. 5) that in the case of heavy H^+, only relatively light H^0 can give good χ^2 fit to the data. Therefore, for fixed values of M_{H^+} and $\tan\beta$ the requirement of $\chi^2 < 19.5$ leads to an *upper bound* on M_H shown in Fig. 6b (where we have optimized the fit with respect to M_A and m_t).

Larger value of χ^2 at the minimum for heavier H^0 observed in Figs. 5 can be explained by the behaviour of the parameter S [31] which was not taken into account in the discussion above. We define S at $q^2 = M_Z^2$ rather than at $q^2 = 0$ (since it is $S(M_Z^2)$ which parametrizes more effectively the electroweak observables measured at LEP):

$$S = \frac{4s_W^2}{\alpha}\left[c_W^2 F_{ZZ}(M_Z^2) - c_W^2 F_{\gamma\gamma}(M_Z^2) + \frac{c_W}{s_W}(2s_W^2 - 1)F_{Z\gamma}(M_Z^2)\right] \quad (13)$$

where

$$F_{ij}(q^2) \equiv \frac{\Pi_{ij}(q^2) - \Pi_{ij}(0)}{q^2} \quad (14)$$

For $q^2 = 0$ it is easy to obtain the analytic expression for $S(0)$ which we record in the Appendix. Since for approximately fixed M_A the parameter S grows with increasing M_H as shown in Fig. 7 it is obvious that for some too high M_H the quality of the fit will be spoiled.

When M_{H^+} increases, its negative contribution decreases S but this decrese is almost entirely compensated

[4] Whenever we optimize with respect to m_t, the top mass measurement $m_t = (173.9 \pm 5)\,\mathrm{GeV}$ [18] is included as one of the data in our χ^2 fit

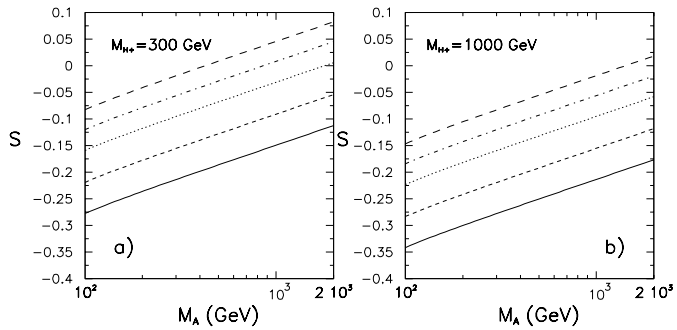

Fig. 7a,b. Parameters S as a function of M_A for $M_{H^+} = 300\,\mathrm{GeV}$ and 1 TeV for $M_H =$ (from below) 100,250,500,1000 and 2000 GeV. In all cases $M_h = 10\,\mathrm{GeV}$ and $\sin^2(\beta-\alpha) = 0$

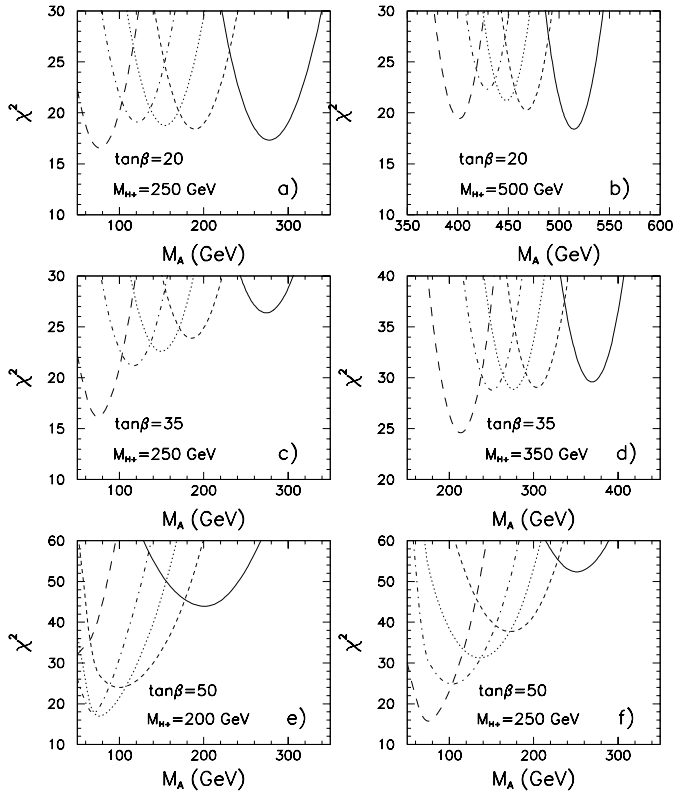

Fig. 8a–f. χ^2 as a function of M_A for three different values of $\tan\beta$ and different H^+ masses for $M_h = 20\,\mathrm{GeV}$ (i.e. $\sin^2(\beta-\alpha) = 0$). Solid, dashed, dotted, dot-dashed and long-dashed lines correspond to M_H =90, 500, 1000, 2000 and 5000 GeV, respectively

by the change in M_A which is required by the $\Delta\rho$ variable so that χ^2 remains in its minimum (for that value of M_{H^+}). Therefore, the upper limit on M_H is, for $\tan\beta \gtrsim 1.5$, almost independent of the assumed value of M_{H^+} as seen in Fig. 6b. For smaller $\tan\beta$, however, lighter H^+ induces larger negative contribution to δR_b and this has the effect that the upper limit on M_H is stronger for lighter H^+ because the minimum of χ^2 is already higher than for heavier H^+. Therefore, this limit is rather stringent for $0.5 \lesssim \tan\beta \lesssim 0.8$.

In the case of light h^0 and $\tan\beta \gtrsim 20$ qualitatively new behaviour of χ^2 appears as a result of the interplay of h^0, A^0 and H^+ contributions to R_b (for $\sin^2(\beta-\alpha) \approx 0$ the H^0 boson contributes negligibly to R_b). Due to tight correlation of M_A with M_{H^+} (required by $\Delta\rho$) acceptable χ^2 cannot be obtained for too heavy H^+ because then there is large negative contribution to R_b due to the large mass spliting between h^0 and A^0. Thus, for large $\tan\beta$ very light h^0 necessarily implies the existence of relatively light H^+. The corresponding pattern of χ^2 (for fixed $m_t = 174\,\mathrm{GeV}$) is illustrated in Fig. 8 for two different values of M_{H^+} and $\tan\beta = 20$, 35 and 50. Deeper minima of χ^2 for larger values of M_H seen in Figs. 8c-f can be explained by the fact that (for fixed M_{H^+}) larger M_H requires lighter A^0 to give acceptable $\Delta\rho$ (the correlation seen already in Fig. 5) and this increases positive contribution to R_b of the latter. From the pattern seen in Fig. 8 it follows that for a given mass of the lighter scalar h^0 and for a given upper bound on M_H there exists an upper bound on M_{H^+}. For $M_h = 20$ and 10 GeV this bound (obtained for $\sin(\beta-\alpha) = 0$ by scanning over M_H, M_A and m_t and looking for points with $\chi^2 < 19.5$) is plotted in Fig. 9a for assumed upper limit on M_H equal 1000, 3000 and 5000 GeV. Taking lighter h^0 strenghten the bound as can be easily inferred from Fig. 4. Of course, for large $\tan\beta$ values allowing for heavier H^0 weakens the upper bound on M_{H^+}. However, for $\tan\beta$ values $\sim 20-30$, where R_b gradually cesses to be so important (even allowing M_H to vary up to 3 TeV), the minimum of χ^2 (for given M_{H^+}) is achieved for $M_H = 90\,\mathrm{GeV}$ (lower limit on the SM-like M_H from direct searches). Therefore the minimum of χ^2 does not depend on the assumed upper limit on M_H. The importance of this upper bound on M_H taken together with the lower one coming from $b \to s\gamma$ is obvious[5].

Since for $\tan\beta \gtrsim 25$ the best χ^2 is obtained for the lowest possible mass of the charged Higgs boson and M_H equal to its assumed upper bound, for given value of $\tan\beta$ there exists a lower bound on M_h which follows from the assumed upper bound on M_H and the lower limit on M_{H^+} coming from $b \to s\gamma$. This bound (obtained by scanning over m_t and M_A as well as over $\sin^2(\beta-\alpha)$ in the experimentally allowed range shown in Fig. 1) is shown in Fig. 9b for two different lower bounds on M_{H^+} taken to be 200 GeV (our limit from $b \to s\gamma$) and 250 GeV and different upper bounds on M_H. (For $M_{H^+} = 200\,\mathrm{GeV}$ the upper limit on M_h does not decrease when larger M_H are allowed because it would require $M_A < 65\,\mathrm{GeV}$ which is excluded by the OPAL analysis, see Fig. 2.) The bound turns out to be very sensitive to the lower limit on M_{H^+} showing that the $b \to s\gamma$ process is crucial for constraining light scalar Higgs scenario for large $\tan\beta$.

The global limits shown in Figs. 9a,b must be confronted with the recent analysis [16] of the Yukawa process

[5] One should note, however, that for given values of the Higgs sector parameters the minimum of χ^2 for $\tan\beta$ close to 50 occurs for $m_t \approx 166\,\mathrm{GeV}$ for which the lower bound on M_{H^+} coming from $b \to s\gamma$ is slightly lower (by about 20 GeV) then the bound plotted in Fig. 6a (which was obtained for fixed $m_t = 174\,\mathrm{GeV}$)

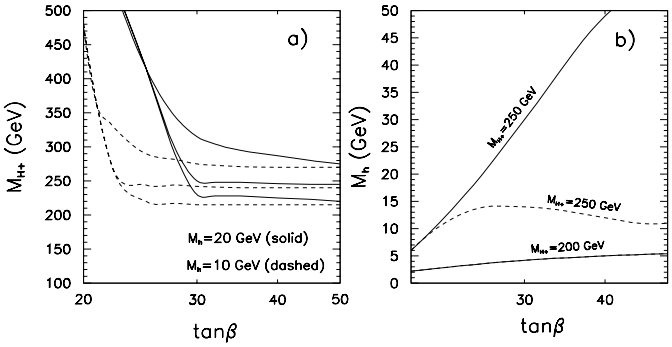

Fig. 9a,b. Limits from the χ^2 fit: **a** Upper for the H^+ mass as a function of $\tan\beta$ for $M_h = 20$ (solid lines) and 10 GeV (dashed lines) assuming the upper limit on M_H equal (from the bottom to top) 1, 3 and 5 TeV. **b** Lower for M_h for M_{H^+} =200 and 250 GeV (solid lines) assuming the upper limit on M_H equal 1 TeV, and for M_{H^+} =250 GeV (dashed line) and $M_H < 3$ TeV

for h^0 production. In the case of Fig. 9a parts of the solid (dashed) lines corresponding to $\tan\beta \gtrsim 40(30)$ seem to be excluded by the data for the Yukawa process. However, not excluded parts of these lines still provide interesting and complementary limits on the light h^0 scenario. In the case of Fig. 9b the limit obtained for $M_{H^+} = 200$ GeV is for most of the $\tan\beta$ range weaker than the limit imposed by the Yukawa process. For heavier H^+ these limits shown in Fig. 9b become competitive to the ones derived in [16].

4.2 Light A^0

In the the case of light A^0 the analysis is more involved because there is effectively one more variable - $\sin^2(\beta-\alpha)$. Let's begin therefore again with the case of triple degeneracy, $M_h = M_H = M_{H^+}$. As is clear from (8) the contribution of the Higgs sector to $\Delta\rho$ is in this limit independent of the value of M_A and of $\sin^2(\beta-\alpha)$ and is given simply by $\Delta\rho_{SM}(M_h)$. Therefore, for $M_h = M_H = M_{H^+}$ and moderate value of $\tan\beta$ ($1.5 \lesssim \tan\beta \lesssim 20$) the best value of χ^2 depends on the lower limit on M_{H^+} from $b \to s\gamma$. For $\tan\beta \gtrsim 1$ the condition $\chi^2 < 19.5$ is satisfied if $M_{H^+} < 240$ GeV which is still allowed (see Fig. 6). For $\tan\beta \lesssim 1$ light H^+ which is needed to give good $\Delta\rho$ tends to give too negative contribution to R_b (see Fig. 6a) and the condition $\chi^2 < 19.5$ cannot be satisfied.

Even for M_{H^+} bigger than 240 GeV, the value of χ^2 can be kept below 19.5 by the departure from the limit of triple degeneracy. For example, consider the limit in which h^0 and H^0 remain degenerate (which makes $\Delta\rho$ independent of $\sin^2(\beta-\alpha)$). It is then easy to see that for any value of M_{H^+} (and any M_A) there exists a solution to the equation $\Delta\rho = 0$ which occurs for $M_h = M_H \lesssim M_{H^+}$. For values of $\tan\beta \lesssim 20$ (for which neutral Higgs bosons do not play any role in R_b) and M_{H^+} not too large (so that the effects of the S parameter are not too large, see below) the existence of such a solution is sufficient to ensure small values of χ^2. Note however that since the solution to the equation $\Delta\rho = 0$ is due to the cancelation of the

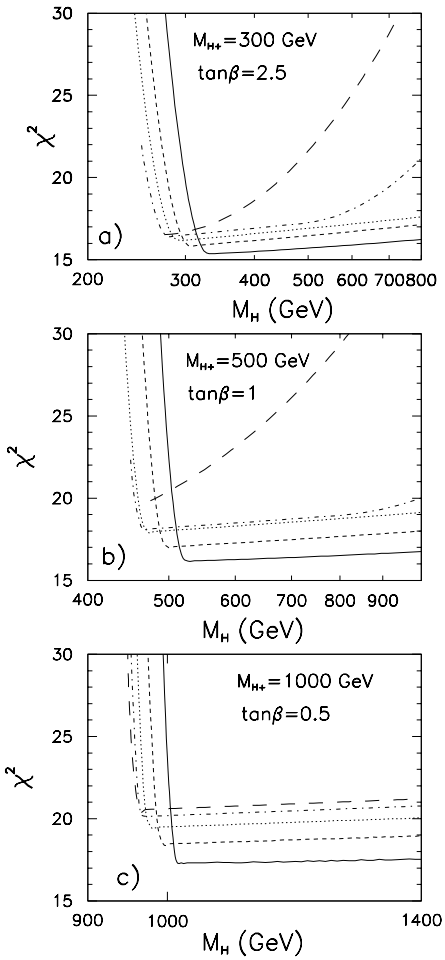

Fig. 10a–c. χ^2 as a function of M_H for different low and intermediate values of $\tan\beta$ and different H^+ masses for M_A = 10 GeV. Solid, dashed, dotted, dot-dashed and long-dashed lines correspond to M_h equal (90, 150, 200, 250, 275) GeV, (90, 200, 400, 450, 475) GeV and (90, 250, 500, 750, 940) GeV for panels **a**, **b** and **c**, respectively

$\Delta\rho_{NEW}$ which depends on the mass splittings qudratically against $\Delta\rho_{SM}(M_h)$ which depends on M_h only logarithmically such a solution is strongly fine-tuned (the more, the heavier H^+). The fine-tuning can be, however, reduced (or, more precisely, shifted to the variable $\sin^2(\beta-\alpha)$) by relaxing the condition $M_h = M_H$. This is illustrated in Fig. 10 where for $M_A = 10$ GeV and $m_t = 174$ GeV we show χ^2 as a function of M_H for different (moderate and low) values of $\tan\beta$ and different choices of M_{H^+} and M_h. In all cases we optimize χ^2 with respect to the value of $\sin^2(\beta-\alpha)$.

The peculiar dependence of χ^2 as a function of M_H seen in Fig. 10 can be understood by inspection of the formulae for $\Delta\rho$, (8). Consider first the case of $M_A = 10$ GeV, $M_{H^+} = 300$ GeV as in Fig. 10a. For $M_h = 90$ GeV and $M_h \lesssim M_H \ll M_{H^+}$ both factors, Δ_c and Δ_s, are positive and obviously cannot cancel the positive first term in (8) for any choice of $\sin^2(\beta-\alpha)$. As M_H increases, however, Δ_s decreases rather fast and takes on negative values for $M_H \lesssim M_{H^+}$ whereas Δ_c decreases slowly (log-

arithmically) and reaches negative values only for very large values of M_H. Obviously, for M_H such that $\Delta_s < -\alpha A(M_A, M_{H^+})/4\pi s_W^2 M_W^2 < \Delta_c$ there always exist a choice of $\sin^2(\beta-\alpha)$ for which $\Delta\rho = 0$. This explains the plateau in χ^2 for light h^0 and $M_H > M_{H^+}$.[6] With M_h increasing Δ_c decreases very fast. In addition Δ_s decreases too, though only logarithmically. As a result, for M_h larger than some critical value both, Δ_c and Δ_s, become negative and smaller than $-\alpha A(M_A, M_{H^+})/4\pi s_W^2 M_W^2$ and again $\Delta\rho$ cannot vanish leading to large values of χ^2 seen in Figs. 10a-c for mass configurations corresponding to dot-dashed and long-dashed lines. It should also be obvious that for very heavy H^+ the fine tuning in $\sin^2(\beta-\alpha)$ becomes extremely big making such solutions rather unnatural. Thus light A^0 and values of $\tan\beta \lesssim 1$, for which M_{H^+} must be large, are rather unlikely.

For very large M_{H^+} $\Delta\rho$ can vanish only for heavy H^0. In the case of heavy h^0 this means that the parameter S is also large (see Fig. 7) and spoils the quality of the fit. This explains why, in Figs. 10c for larger values of M_h, and even for the other masses in configurations for which $\Delta\rho$ can vanish due to a judicious adjustment of $\sin^2(\beta-\alpha)$, the value of χ^2 is still above 19.5.

From the above explanation it is clear that for small and intermediate values of $\tan\beta$ a light $CP-$odd scalar A^0 can be tolerated provided h^0 is lighter than some bound M_B which is only slightly smaller than the mass of the charged Higgs boson (which in turn is constrained by $b \to s\gamma$ and, for $\tan\beta < 1$ by the R_b measurements). At the same time, M_H is bounded from below also by roughly the same mass M_B. Of course, according to our previous discussion, the case $M_h = M_H \lesssim M_{H^+}$ is always allowed (in this case $\sin^2(\beta-\alpha)$ is completely unconstrained). It is also worth noting that for $M_h \ll M_H \approx M_B \approx M_{H^+}$ the value of $\sin^2(\beta-\alpha)$ (which is crucial for h^0 and A^0 production processes) needed to keep χ^2 below 19.5 is close to 1, implying that in this case M_h is constrained by the LEP search to be greater than $\approx 90\,\mathrm{GeV}$. For heavier H^0, $\sin^2(\beta-\alpha)$ decreases which means that the experimental lower bound on M_h is also relaxed appropriately (recall that the limits from the associated h^0A^0 production require only $M_h \gtrsim 50\ (70)\,\mathrm{GeV}$ for $M_A = 10\ (50)\,\mathrm{GeV}$ - see Fig. 2 - irrespectively of the value of $\sin^2(\beta-\alpha)$). The decrease of $\sin^2(\beta-\alpha)$ with $M_H > M_{H^+}$ is slightly faster for heavier A^0 (and/or h^0) and slower for heavier H^+.

For large $\tan\beta$ the dependence of χ^2 on M_H for different values of M_h and M_{H^+} is shown in Fig. 11. The mass of the $CP-$odd scalar is taken to be 25 GeV in order to respect the bound from the Yukawa process also for $\tan\beta = 50$ [15,16]. The behaviour of χ^2 can be explained combining the information contained in Figs. 10 (reflecting mainly the behaviour of $\Delta\rho$) with the behaviour of the corrections to R_b for different Higgs boson mass configurations. In order not to have too negative corrections to the latter quantity the neutral scalar which couples more strongly to the $b\bar{b}$ pair cannot be too heavy. On the other hand, for $M_H \lesssim M_{H^+}$ good $\Delta\rho$ is obtained for $\sin^2(\beta-\alpha) \approx 1$ (i.e. $\sin\alpha \approx 0$) which means that it is the mass splitting between H^0 and A^0 which is relevant for R_b. Only for sufficiently heavy H^0 does $\sin^2(\beta-\alpha)$ become small enough ($\sin\alpha \approx 1$) so that h^0 couples with full strenght to $b\bar{b}$, and becomes relevant for R_b. Thus, a good fit to the data can be obtained only with light h^0 and rather heavy H^0 (since this occurs for $\sin^2(\beta-\alpha) \ll 1$, h^0 can be lighter than 90 GeV as we have just explained). The increase of χ^2 for $M_H > 1\,\mathrm{TeV}$ seen in Fig. 11a and d for $M_h = 70$ and 90 GeV is due to the fact that for lighter H^+ Δ_c becomes smaller than $-\alpha A(M_{H^+}, M_A)/4\pi s_W^2 M_W^2$ already for relatively light H^0. Since, as explained above, Δ_c decreases very fast as M_h increases, this effect is even more pronounced for $M_h = 150\,\mathrm{GeV}$. Note that because of this effect for $M_{H^+} = 200\,\mathrm{GeV}$ one can reach $\chi^2 < 19.5$ only for $M_h < 90\,\mathrm{GeV}$.

For the same value of M_H and M_h the χ^2 is slightly bigger for heavier H^+ (despite the fact that negative contribution of the latter Higgs boson to R_b is decreased) because of the behaviour of $\sin^2(\beta-\alpha)$: it is larger for heavier H^+ and therefore light h^0 does not fully compensate for the effects of light A^0 as h^0 couples weaker to the $b\bar{b}$ pair. The conclusion following from the above considerations and from Figs. 11 is that in the scenario with large $\tan\beta$ and light $CP-$odd neutral Higgs particle ($M_A \gtrsim 25\,\mathrm{GeV}$) the mass of the lighter neutral $CP-$even

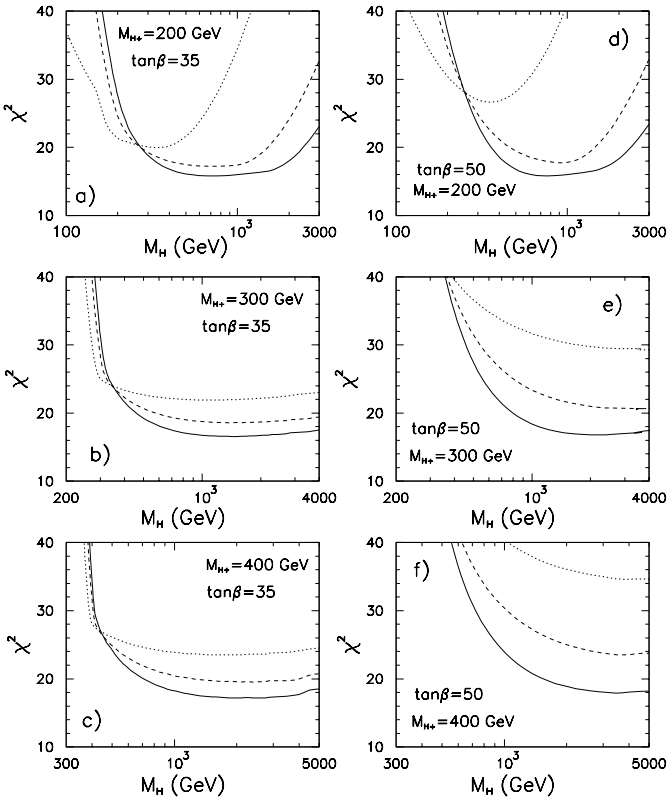

Fig. 11a–f. χ^2 as a function of M_H for $\tan\beta = 35$ and 50 and different H^+ masses. Solid, dashed, dotted, lines correspond to M_h equal 70, 90 and 150, respectively. $M_A = 25\,\mathrm{GeV}$

[6] Eventually, for M_H large enough, also Δ_c becomes smaller than $-\alpha A(M_A, M_{H^+})/4\pi s_W^2 M_W^2$ so that there is again no solution with $\Delta\rho = 0$. This happens for smaller M_H the smaller is the value of M_{H^+}

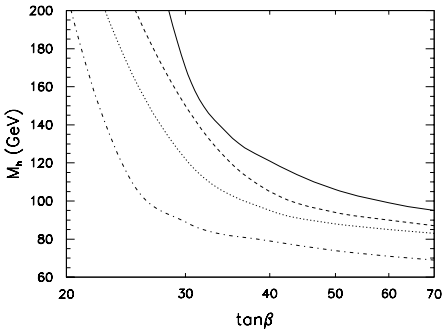

Fig. 12. Upper limit on M_h in the light $CP-$odd scalar scenario as a function of $\tan\beta$ for M_A =25 GeV (solid line), 15 GeV (dashed line), 10 GeV (dotted line) and 1 GeV (dot-dashed line)

boson, h^0 is bounded from above. This upper bounds on M_h for four different values of the light $CP-$odd scalar mass (obtained by scanning over m_t, $\sin(\beta-\alpha)$, M_H and M_{H^+}) are show as functions of $\tan\beta$ in Fig. 12. Of course, as $\tan\beta$ decreases the upper limit on M_h approaches the bound $M_B \lesssim M_{H^+}$ discussed previously. The existence of an upper bound on M_h means that the LEP2 will be able to effectively test the scenario with light A^0 and large $\tan\beta$ either via Bjorken process or the associated Higgs boson production, at least for $\tan\beta > 45(30)$ for $M_A < 25(10)$ GeV.

5 Summary of the results of the global fit and other constraints

We have investigated the impact the precision electroweak data have on the parameter space of the 2HDM of type II. We have been particularly interested in constraints imposed on the very light neutral scalar scenarios (with h^0 or A^0 in the range $\lesssim 25-30$ GeV) by the requirement of good (as good as in the SM) fit to the electroweak data. It turns out that both scenarios are not excluded (neither directly nor indirectly) provided some constraints are respected.

Apart from the well known constraints on the charged Higgs boson mass set in 2HDM (II) by $b \to s\gamma$ and, for $\tan\beta < 1$, by R_b we find that in the case of light $CP-$even scalar, h^0, and intermediate values of $\tan\beta$ in order to maintain in the 2HDM(II) the same quality of the χ^2 fit to the data as in the SM, masses of the $CP-$odd and charged Higgs bosons must be tightly correlated (the more, the heavier is H^+) leading to strong "fine-tuning" of this scenario. Therefore, limiting the acceptable degree of "fine-tuning" yields an upper bound on M_{H^+} (Fig. 6a). For a given mass of H^+ the requirement of the good fit to the data puts also an upper limit on M_H which is particularly strong for $\tan\beta < 1$ (Fig. 6b). For large values of $\tan\beta$ ($\tan\beta \gtrsim 20-30$) the interplay between the corrections to $\Delta\rho$ and R_b implies that if h^0 is light, H^+ must be also light. The upper limit (as a function of $\tan\beta$) depends on the assumed upper bound on M_H but for M_H in the TeV range is very strong for $\tan\beta \gtrsim 35$, M_{H^+} of order of 300 GeV (Fig. 9a). It is also interesting that for large $\tan\beta$ and $M_{H^+} > 200$ GeV the electroweak data set the lower limit on the mass of h^0 shown in Fig. 9b.

For the light A^0 scenario we find that for low and intermediate values of $\tan\beta$ the quality of the fit is maintained provided $M_h < M_B < M_H$ where $M_B \lesssim M_{H^+}$. For $\tan\beta > 30-35$ there emerges an additional upper bound on the mass of the lighter scalar h^0 which enables the test of the light A^0-large $\tan\beta$ configuration at LEP2.

Other potential sources of further constraints on the 2HDM(II) which we have not considered here are the muon $g-2$ measurement [34] and $Z \to h(A)\gamma$ decays [35].

The upper limit on $BR(Z^0 \to h^0(A^0)\gamma)$ decays set by LEP1 constrain our model only for $h^0(A^0)$ masses below 20 GeV and for values of $\tan\beta$ either very low (below 0.2) or very large, above $55-70$ GeV (which we have not considered). For larger $h^0(A^0)$ masses $\tan\beta$ is pushed outside the range (6) in which perturbative calculations can be done reliably. In this case, the resulting constraints can eventually be given a meaning as constraining the effective (on-shell) $Z^0h^0\gamma$ and $Z^0A^0\gamma$ couplings but the relation of these coupling to the original parameters of the model (which we have been using) cannot be calculated perturbatively.

The constraints following from the present measurement of $g-2$ of the muon are stronger than the ones following from the Yukawa process only for $h^0(A^0)$ masses below $1-2$ GeV in which case they exclude values of $\tan\beta \gtrsim 4(10)$ for $M_{h(A)} = 0.1(1)$ GeV. The E821 experiment may (depending on the measured central value) improve these limits (according to analysis presented in [34]) so that they become stronger than the Yukawa process ones up to $M_{h(A)} \sim 10$ GeV and exclude values of $\tan\beta \gtrsim 2(15)$ for $M_{h(A)} = 1(10)$ GeV.

Acknowledgements. P.H.Ch. has been partly supported by the Polish State Committee for Scientific Research grant 2 P03B 030 14 (for 1998-1999). M.K. has been partly supported by the U.S.-Polish Maria Skłodowska-Curie Joint Fund II (MEN/DOE-96-264) and by the Polish State Committee for Scientific Research grants 2 P03B 014 14 and 2 P03B 184 10. We would like to thank F. Borzumati, C. Greub and M. Misiak for discussions. M.K. would also like to thank J. Gunion and W. Hollik for important suggestions, H. Haber for discussions and hospitality during her stay at the Santa Cruz University and K. Desh for providing some experimental data.

Appendix

Here we give the expression for the parameter $S(0)$. It differs slightly from the formula presented in [36].

$$S = -\frac{1}{6\pi}\log\frac{M_{H^+}}{M_W} + \frac{1}{\pi}\sin^2(\beta-\alpha)\big[A'(M_A,M_H) + A'(M_W,M_h) + M_Z^2B'(M_Z,M_h)\big] + \frac{1}{\pi}\cos^2(\beta-\alpha) \times \big[A'(M_A,M_h) + A'(M_W,M_H) + M_Z^2B'(M_Z,M_H)\big]$$

The functions A' and B' are given by:

$$A'(m_1,m_2) = \frac{1}{12}\left[-\frac{11}{6} + \frac{m_1^2}{m_1^2-m_2^2}\log\frac{m_1^2}{M_W^2} + \frac{m_2^2}{m_2^2-m_1^2}\log\frac{m_2^2}{M_W^2} + \frac{m_1^4+m_2^4}{(m_1^2-m_2^2)^2} - \frac{m_1^2m_2^2(m_1^2+m_2^2)}{(m_1^2-m_2^2)^3}\log\frac{m_1^2}{m_2^2}\right]$$

$$B'(m_1,m_2) = -\frac{1}{2}\frac{m_1^2+m_2^2}{(m_1^2-m_2^2)^2} + \frac{m_1^2m_2^2}{(m_1^2-m_2^2)^3}\log\frac{m_1^2}{m_2^2}$$

References

1. The LEP Electroweak Working Group, CERN report LEPEWWG/99-0.1.
2. M. Krawczyk, in proceedings of the *XXXI Rencontres de Moriond* "Electroweak Interactions and Unified Theories" Les Arcs, France, March 1996, ed. Tran Than Van, World Scienific, (hep-ph/9607268), Proceedings of the *XXVIII Rochester Int. Conf. on High Energy Physics*, Warsaw, Poland, July 1996, eds. Z. Ajduk, A.K. Wróblewski, World Scientific, p. 1460, Proceedings of the *Cracow School of Theoretical Physics*, Zakopane, Poland, January 1999, *Acta Phys. Pol.* **B29** (1999) 3543.
3. A.K. Grant, *Phys. Rev.* **D51** (1995) 207.
4. W.F.L. Hollik, *Z. Phys.* **C32** (1986) 291; **C37** (1988) 568.
5. H.E. Haber and K. Logan, talk at the *First European Meeting From Planck Scale to Electroweak Scale*, Kazimierz, Poland, May 1998.
6. F. Cornet, W.F.L. Hollik and W. Mösle *Nucl. Phys.* **B428** (1994) 61.
7. J.F. Gunion, H.E. Haber, G.L. Kane and S. Dawson, *The Higgs Hunters Guide*, Addison-Wesley, 1990.
8. H. Haber, in *Perspectives on Higgs Physics II*, ed. G.L. Kane, World Scientific, 1998 (hep-ph/9707213).
9. V. Berger et al., *Phys. Rev.***D41** (1990) 3421; Y. Grossman, *Nucl. Phys.* **B426** (1994) 355.
10. ALEPH Collaboration, ALEPH 98-029 CONF 98-017; K. Moenig for the DELPHI Collaboration talk at the LEPC Meeting, CERN, March 31, 1998; M. Acciarri et al. (the L3 Collaboration), preprint CERN-EP/98-052; OPAL Physics Note PN340, March 1998; V. Ruhlmann-Kleider, Talk at the *XXX Rencontres de Moriond* "QCD and Hadronic Interactions" Les Arcs, France, March 1998; M. Felcini talk at the *XXXIV Rencontres de Moriond* "Electroweak Interactions and Unified Theories" Les Arcs, France, March 1999
11. Abaldin et al. (the OPAL Collaboration), *Eur. J. Phys.* **C7** (1999) 407.
12. M. Acciari et al. the (L3 Collaboration), *Z. Phys.* **C62** (1994), 551, paper PA11-016 submited to the *XXVIII Rochester Int. Conf. on High Energy Physics*, Warsaw, Poland, July 1996.
13. F. Wilczek *Phys. Rev. Lett.* **39** (1977) 1304.
14. P. Lee-Franzini, in Proceedings of the *XXIV Rochester Int. Conf. on High Energy Physics*, Munich, Germany 1988, eds. R. Kotthaus and J. H. Kühn, p. 1432; M. Narain, Ph.D. Thesis, *Inclusive photon spectra from* Υ, State Univ. of New York at Stony Brook, 1991; S. T. Lowe, Ph.D.Thesis, *A search for narrow states in radiative* Υ *decays*, SLAC, 1986; D. Antreasyan et al. (the Crystall Ball Collaboration), *Phys. Lett.* **B251** (1990) 204.
15. The ALEPH Collaboration, paper PA13-027 submited to the *XXVIII Rochester Int. Conf. on High Energy Physics*, Warsaw, Poland, July 1996.
16. P. Zalewski, private communication
17. M. Felcini, talk at the *XXXIV Rencontres de Moriond* "Electroweak Interactions and Unified Theories" Les Arcs, France, March 1999; B. Bevensee, Proceedings of the *XXXIII Rencontres de Moriond* "Electroweak Interactions and Unified Theories" Les Arcs, France, March 1998, ed. Tran Than Van, World Scienific (preprint FERMILAB-CONF-98-1555-E).
18. M. Jones (for the D0 and CDF Collaborations) talk at the *XXXIII Rencontres de Moriond* (Electroweak Interactions and Unified Theories), Les Arcs, France, March 1998.
19. J. Ellis, G.L. Fogli and E.Lisi, *Phys. Lett.* **B389** (1996) 321 and references therein; P.H. Chankowski and S. Pokorski, *Phys. Lett.* **B356** (1995) 307 and hep-ph/9509207.
20. P.H. Chankowski and S. Pokorski, *Phys. Lett.* **B366** (1996) 188, and in *Perspectives on Supersymmetry*, ed. G.L. Kane, World Scientific, Singapore (hep-ph/9707497); W. de Boer, A. Dabelstein, W.F.L. Hollik, W. Mösle and U. Schwickerath, *Z. Phys.* **C75** (1997) 627 and preprint IEKP-KA-96-08 (hep-ph/9609209).
21. G. Altarelli, R. Barbieri and S. Jadach, *Nucl. Phys.* **B396** (1992) 3; J.L. Hewett, T. Takeuchi and S. Thomas, preprint SLAC-PUB-7088 (hep-ph/9603391) in *Electroweak Symmetry Breaking and Beyond the Standard Model* ed. by T. Barklow, S. Dawson, H.E. Haber and S. Siegriest, World Scientific, Singapore.
22. J. Rosiek *Phys. Lett.* **B252** (1990) 135; A. Denner, R.J. Guth, W.F.L. Hollik and J.H. Kühn, *Z. Phys.* **C51** (1991) 695; M. Boulware and D. Finnell, *Phys. Rev.* **D44** (1991) 2054.
23. P.H. Chankowski and S. Pokorski *Nucl. Phys.* **B475** (1996) 3.
24. The CLEO Collaboration, paper ICHEP98 1011 submitted to the *XXIX Rochester Int. Conf. on High-Energy Physics*, Vancouver, B.C., Canada, 1998, (preprint CLEO CONF 98-17).
25. A.J. Buras, M. Misiak, M. Münz, S. Pokorski *Nucl. Phys.* **B424** (1994) 374.
26. K. Adel and Y.P. Yao, *Phys. Rev.* **D49** (1994) 4945; C. Greub, T. Hurth and D. Wyler, *Phys. Lett.* **B380** (1996) 385 and *Phys. Rev.* **D54** (1996) 3350.
27. M. Ciuchini, G. Degrassi, P. Gambino and G.-F. Giudice, *Nucl. Phys.* **B527** (1998) 21; P. Ciafaloni, A. Romanino and A. Strumia, *Nucl. Phys.* **B524** (1998) 361.
28. A. Czarnecki and W.A. Marciano *Phys. Rev. Lett.* **81** (1998), 277; A. Kagan and M. Neubert, *Eur. Phys. J.* **C7** (1999) 5.
29. K. Chetyrkin, M. Misiak and M. Münz, *Phys. Lett.* **B400** (1997) 206.
30. C. Greub and F.M. Borzumati, talk by C.G. at the *XXIX Int. Conf. on High Energy Physics*, Vancouver, B.C., Canada, Jul. 1998, (hep-ph/9810240).
31. M. Peskin and T. Takeuchi *Phys. Rev. Lett.* **65** (1990), 964, *Phys. Rev.* **D46** (1992) 381.
32. A. C. Bawa, and M. Krawczyk, Contribution to the HERA Working Group, Warsaw preprint IFT 16/91 and Erratum; IFT 17/93; *Phys. Lett.* **B 357** (1995) 637; M. Krawczyk, Proceedings of the Workshop *Future Physics at HERA*, 1995-96, p. 244 (hep-ph/9609477).

33. J. Kalinowski and M. Krawczyk, *Phys. Lett.* **B361** (1995) 66, *Acta Phys. Pol.* **B27** (1996) 961.
34. M. Krawczyk and J. Żochowski, *Phys. Rev.* **D55** (1997) 6968.
35. M. Krawczyk, P. Mättig and J. Żochowski, *Eur. Phys. J.* **C8** (1999) 495.
36. T. Inami, C.S. Lim and A. Yamada, *Mod. Phys. Lett.* **A7** (1992) 2789.